Endothelial Cell-surface gp60 Activates Vesicle Formation and Trafficking via G_i-coupled *Src* Kinase Signaling Pathway

Richard D. Minshall,* Chinnaswamy Tiruppathi,* Stephen M. Vogel,* Walter D. Niles,* Annette Gilchrist,‡ Heidi E. Hamm,‡ and Asrar B. Malik*

*Department of Pharmacology, University of Illinois, College of Medicine, Chicago, Illinois 60612; and ‡Department of Pharmacology and Molecular Biology, Northwestern University School of Medicine, Chicago, Illinois 60611

Abstract. We tested the hypothesis that the albumin-docking protein gp60, which is localized in caveolae, couples to the heterotrimeric GTP binding protein G_i, and thereby activates plasmalemmal vesicle formation and the directed migration of vesicles in endothelial cells (ECs). We used the water-soluble styryl pyridinium dye *N*-(3-triethylaminopropyl)-4-(p-dibutylaminostyryl) pyridinium dibromide (FM 1-43) to quantify vesicle trafficking by confocal and digital fluorescence microscopy. FM 1-43 and fluorescently labeled anti-gp60 antibody (Ab) were colocalized in endocytic vesicles within 5 min of gp60 activation. Vesicles migrated to the basolateral surface where they released FM 1-43, the fluid phase styryl probe. FM 1-43 fluorescence disappeared from the basolateral EC surface without the loss of anti-gp60 Ab fluorescence. Activation of cell-surface gp60 by cross-linking (using anti-gp60 Ab and secondary Ab) in EC grown on microporous filters increased transendothelial ^{125}I-albumin permeability without altering liquid permeability (hydraulic conductivity), thus, indicating the dissociation of hydraulic conductivity from the albumin permeability pathway. The findings that the sterol-binding agent, filipin, prevented gp60-activated vesicle formation and that caveolin-1 and gp60 were colocalized in vesicles suggest the caveolar origin of endocytic vesicles. Pertussis toxin pretreatment and expression of the dominant negative construct encoding an 11–amino acid $G_{\alpha i}$ carboxyl-terminal peptide inhibited endothelial ^{125}I-albumin endocytosis and vesicle formation induced by gp60 activation. Expression of dominant negative *Src* (dn-*Src*) and overexpression of wild-type caveolin-1 also prevented gp60-activated endocytosis. Caveolin-1 overexpression resulted in the sequestration of $G_{\alpha i}$ with the caveolin-1, whereas dn-*Src* inhibited $G_{\alpha i}$ binding to caveolin-1. Thus, vesicle formation induced by gp60 and migration of vesicles to the basolateral membrane requires the interaction of gp60 with caveolin-1, followed by the activation of the downstream G_i-coupled *Src* kinase signaling pathway.

Key words: transcytosis • endocytosis • caveolae • microvascular endothelial cells • albumin permeability

Introduction

Albumin is the primary plasma protein that maintains the colloid osmotic pressure gradient across the semi-permeable microvascular endothelial barrier and, hence, the plasma interstitial albumin concentration gradient is critical in regulating tissue fluid balance (for review see Lum and Malik, 1994). A transcellular pathway through endothelial cells has been implicated in the transport of albumin (Ghitescu et al., 1986; Milici et al., 1987; Shasby and Peterson, 1987; Michel, 1992), lipids, hormones, peptides, and drugs that bind avidly to albumin (Peters, 1975; Partridge, 1979; Forker and Luxton, 1983). The endothelial cell surface 60-kD glycoprotein, gp60[1] or albondin (Schnitzer et al., 1988; Ghinea et al., 1989; Schnitzer and Oh, 1994; Tiruppathi et al., 1996), is believed to be important in the mechanism of albumin binding and activation of transcellular albumin transport via vesicles. Albumin can also cross the endothelial barrier via a diffusional-convective paracellular pathway (Lum and Malik, 1994). Inflammatory

Address correspondence to Asrar B. Malik, Department of Pharmacology, University of Illinois, College of Medicine, 835 South Wolcott Avenue (M/C 868), Chicago, IL 60612. Tel.: (312) 996-7635. Fax: (312) 996-1225. E-mail: abmalik@uic.ed

[1]*Abbreviations used in this paper:* Ab, antibody; BLMVEC, bovine lung microvessel endothelial cells; cav-1, caveolin-1; DAPI, 4′,6-diamidino-2-phenylindole, dihydrochloride; dn-*Src*, dominant negative *Src*; EC, endothelial cell; FM 1-43, *N*-(3-triethylaminopropyl)-4-(p-dibutylaminostyryl) pyridinium dibromide; GFP, green fluorescent protein; gp60, 60-kD albumin-docking protein; L_p, hydraulic conductivity; LSM, laser scanning microscope; RH 414, *N*-(3-triethylammoniumpropyl)-4-(4-(4-(diethylamino)phenyl) butadienyl)pyridinium dibromide; RT-PCR, reverse transcription–PCR.

mediators such as thrombin and histamine increase endothelial albumin permeability by increasing the size of interendothelial clefts (Majno et al., 1969; Garcia et al., 1986; Del Vecchio et al., 1987; Qiao et al. 1995; Rabiet et al., 1996).

We purified gp60 from pulmonary microvascular endothelial cells and showed it could bind specifically and in a saturable manner to albumin (Tiruppathi et al., 1996). We also showed that activation of the cell-surface gp60 using a cross-linking antibody (Ab) induced the transendothelial flux of albumin (Tiruppathi et al., 1997). Inhibitor studies suggested the increased albumin flux involved the activation of *Src* family tyrosine kinases that phosphorylated caveolin-1 and gp60 (Tiruppathi et al., 1997). Formation of vesicles induced by gp60 was inhibited by the tyrosine kinase inhibitors, herbimycin A and genistein (Tiruppathi et al., 1997; Niles and Malik, 1999). Trafficking of vesicles to the basolateral membrane in endothelial cells also required the *N*-ethylmaleimide–sensitive fusion factor (NSF) and soluble NSF attachment protein receptor (Niles and Malik, 1999).

The heterotrimeric GTP binding protein, G_i, binds to caveolin-1 in the caveolar membrane (Li et al., 1995; Okamoto et al., 1998) and activates *Src* kinases (Luttrell et al., 1996; Igishi and Gutkind, 1998; Ellis et al., 1999), which also bind to caveolin-1 (Li et al., 1996). Since gp60 is localized in the caveolar membrane (Schnitzer and Oh, 1994) and is capable of activating *Src* family tyrosine kinases (Tiruppathi et al., 1997), we addressed the possible role of the $G_{\alpha i}$-coupled *Src* kinase pathway in gp60-activated signaling vesicle formation and trafficking in endothelial cells.

Materials and Methods

Antibodies

gp60 Ab was prepared as described previously (Tiruppathi et al. (1996). Polyclonal anti-gp60 Ab was labeled with the Cy3 bisfunctional reactive dye (Tiruppathi et al., 1997). Monoclonal and polyclonal anti–caveolin-1 antibodies were obtained from Transduction Laboratories. Rabbit-anti-$G_{\alpha i}$ polyclonal Ab recognizing the carboxyl-terminal region of isoforms 1 and 2 (KNNLKDCGLF) was purchased from Calbiochem. Goat anti–rabbit and anti–mouse IgG labeled with rhodamine, FITC, Alexa 568, or Alexa 488 and BSA-Alexa 488 conjugate were purchased from Kirkegaard & Perry Laboratories and Molecular Probes, Inc.

Fluorescent Probes

We used fluorescent water-soluble styryl pyridinium dyes *N*-(3-triethylaminopropyl)-4-(p-dibutylaminostyryl) pyridinium dibromide (FM 1-43) and *N*-(3-triethylammoniumpropyl)-4-(4-(4-(diethylamino)phenyl) butadienyl) pyridinium dibromide (RH 414; Molecular Probes, Inc.) to label plasmalemma-derived vesicles (Niles and Malik, 1999). Stock solutions of 5 mg/ml were prepared in DMSO and stored in a desiccator at −80°C for up to 1 mo. Cell staining solutions (5 μg/ml) were made in HBSS containing 20 mM Hepes, 2 mM Ca^{2+}, and 2 mM Mg^{2+}. Staining solutions and subsequent washing buffer contained fixed BSA concentration (6 mg/ml; fraction V, 99% pure, endotoxin-free; Sigma Chemical Co.).

Albumin Iodination

BSA was labeled with $Na^{125}I$ (New England Nuclear) using the chloramine T procedure (Bocci, 1964). Free iodine-125, separated from ^{125}I-albumin with a Sephadex G25 column, constituted <0.3% of the total radioactivity.

Endothelial Cell (EC) Cultures

Bovine lung microvessel ECs (BLMVEC) were isolated and cultured in high glucose DME (GIBCO BRL) supplemented with 10% FBS (Hyclone), 5 mM glutamine, 50 U/ml penicillin, and 50 μg/ml streptomycin (Del Vecchio et al., 1992). Endothelial cell cultures were maintained in an incubator at 37°C in 5% CO_2/95% room air.

Plasmid DNA Preparations

Wild-type (wt) caveolin-1 was prepared from human umbilical vein ECs endothelial cells by reverse transcription–PCR (RT-PCR). The sequenced RT-PCR product was identical to human caveolin-1. The RT-PCR product was subcloned into pcDNA3.1 (Invitrogen) and used for transfection studies. Dominant negative *Src* (dn-*Src*) (Y527F, K295M) and wt-*Src* in vector pSM were obtained from Dr. Silvio Gutkind (National Institute of Dental Research, National Institutes of Health, Bethesda, MD). $G_{\alpha i}$ and $G_{\alpha q}$ dominant negative minigenes encoding the 11–amino acid carboxyl terminus of $G_{\alpha i}$ (IKNNLKDCGLF) or $G_{\alpha q}$ (LQLNLKEYNAV; Gilchrist et al., 1998) were ligated into pcDNA3.1 plasmid vector. A minigene encoding a scrambled sequence of $G_{\alpha i}$ (NGIKCLSNDKL) was used as a negative control. Green fluorescent protein (GFP) plasmid DNA (plasmid pGREEN LANTERN-1) was purchased from GIBCO BRL.

^{125}I-Albumin Endocytosis

Endocytosis of ^{125}I-albumin was measured as described previously (Tiruppathi et al., 1997). BLMVEC were grown to confluence in either 6- or 12-well culture plates. Monolayers were washed twice with 10 mM Hepes-buffered DME, pH 7.4, and the uptake of ^{125}I-albumin was carried out for 25 min at 37°C. Endocytosis was terminated by placing EC monolayers on ice and washing three times with either pH 2.5 buffer (0.2 M acetic acid and 0.5 M NaCl) or pH 3.0 buffer (20 mM glycine-HCl and 0.15 M NaCl) to remove the surface-bound ^{125}I-albumin (Tiruppathi et al., 1992). Cells were lysed with 50 mM Tris-HCl buffer, pH 7.4, containing 1% Triton X-100 and 0.5% SDS, and the lysate was used to measure endocytosis of ^{125}I-albumin.

Transendothelial ^{125}I-Albumin Permeability

Transendothelial ^{125}I-BSA permeability of BLMVEC monolayers grown on microporous polycarbonate transwell filter inserts (Corning Costar Corp.) was measured as previously described (Del Vecchio et al., 1987; Siflinger-Birnboim et al., 1988).

Endothelial Monolayer Hydraulic Conductivity (L_p)

Confluent BLMVEC on gelatin-coated microporous polycarbonate filters were used to measure transendothelial fluid flux using the two-compartment system (Qiao et al., 1993). Both upper and lower chambers were filled with 0.5% albumin in HBSS, pH 7.4, at 37°C and sealed with rubber stoppers. Constant flow perfusion was used to renew the luminal fluid every minute and to prevent an increase in osmolarity. Hydrostatic pressure in the upper chamber was controlled by adjusting the height of the outflow tubing. The filtrate was collected in 1-min intervals and the filtration rate per unit surface (Jv [$\times 10^{-6}$ ml/cm^2/s]) was calculated by measuring the timed movement of fluid meniscus in the collecting tubing. The filtration rate at the two given pressures (P_1 = 0 cm H_2O and P_2 = 5 cm H_2O) at 20-min intervals was measured for up to 2 h. The L_p was calculated as $(Jv_1 - Jv_2)/(P_1 - P_2)$ (Qiao et al., 1993).

Cell-surface gp60 Cross-linking

BLMVEC monolayers were washed twice with Hepes-buffered DME (at 4°C) and incubated with 10 μg/ml of anti-gp60 Ab, followed by 10 μg/ml of a secondary Ab (goat anti–rabbit) for 30 min at 4°C (Tiruppathi et al., 1997). After treatment, the cells were rewarmed to 37°C for the experiments.

Styryl Pyridinium Dye Uptake

Endocytosis in endothelial cells was quantified as described previously (Niles and Malik, 1999) using the styryl pyridinium dyes, FM 1-43 and RH 414. In brief, 5×10^4 BLMVEC were plated on 25-mm-diam No. 1 coverslips or Lab-tek chamber slides (Nalge Nunc Intl.) coated with 0.1% gelatin. Cells were incubated in buffered medium containing 5 μg/ml FM 1-43 or RH 414 at 37°C for 15 min, and then washed three times in ice-cold HBSS. As styryl pyridinium dyes fluoresce brightly at the membrane–water interface (Betz et al., 1992), FM 1-43 fluorescence associated with the cells after washing cell surface probe was the result of incorporation of FM 1-43 into plasmalemma-derived vesicles.

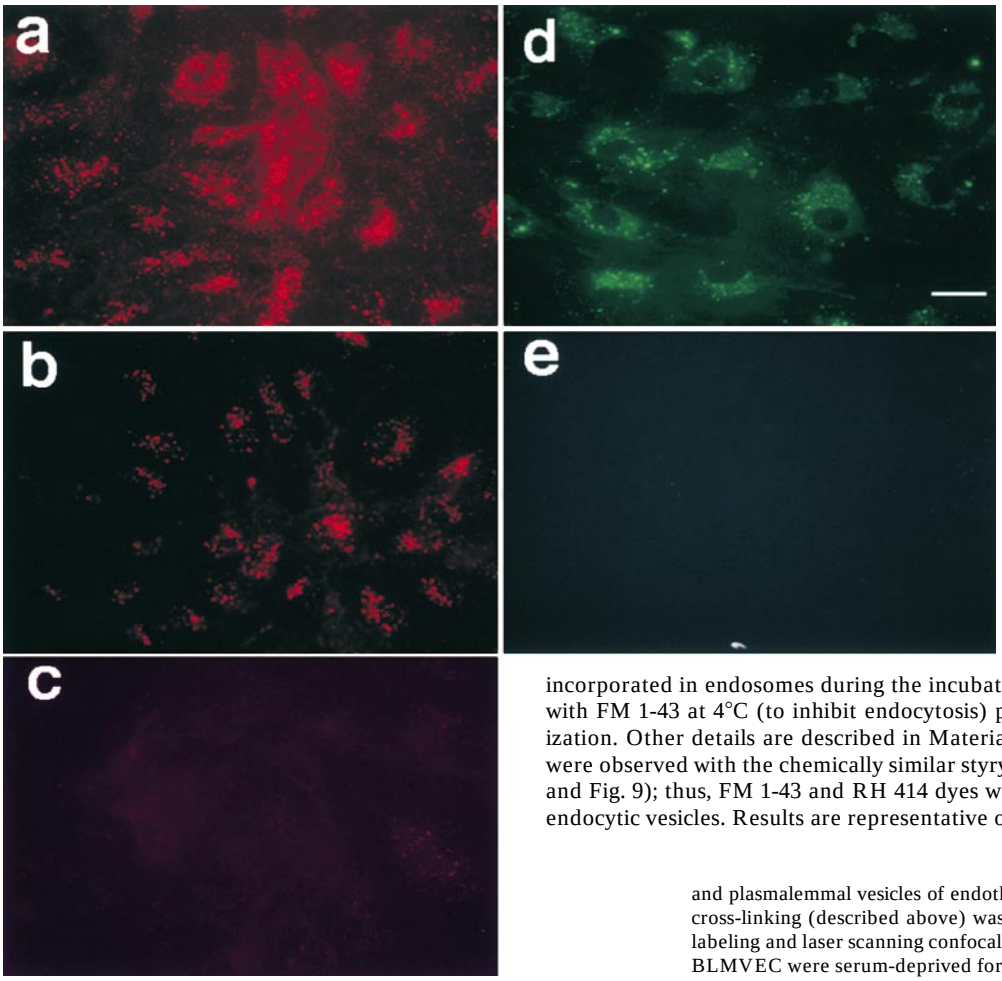

Figure 1. Labeling of gp60 and endocytic vesicles in live endothelial cells. (a) BLMVEC were incubated with Cy3-labeled anti-gp60 Ab at 37°C for 15 min and washed at a low temperature (4°C) to label gp60; red fluorescent images reflect cell surface and internalized fluorescence. (b) Cells were treated identically to a, except that cells were washed with a low pH (3.0) fluid to show internalized gp60. (c) Control photomicrograph only shows background staining when incubation was carried out at 4°C and washed with pH 3.0 buffer. (d) Cells were incubated for 15 min at 37°C with FM 1-43 and washed at normal pH with dye-free buffer to label endosomes; green fluorescence indicates FM 1-43 incorporated in endosomes during the incubation period. (e) 15-min incubation with FM 1-43 at 4°C (to inhibit endocytosis) prevents fluorescent dye internalization. Other details are described in Materials and Methods. Identical results were observed with the chemically similar styryl dye, RH 414 (as shown in Fig. 8 and Fig. 9); thus, FM 1-43 and RH 414 dyes were used interchangeably to label endocytic vesicles. Results are representative of five experiments. Bar, 20 μm.

Digital Fluorescent Microscopy

Live cell fluorescent imaging was performed with an inverted Nikon microscope as previously described (Niles and Malik, 1999). Fluorescence and differential interference contrast images were recorded for each cell field with a cooled integrating charge-coupled device camera (Imagepoint; Photometrics). Quantitative analysis of images (median cell brightness and the number of particles per cell) was performed using Image Pro Plus software with custom written functions as previously described (Niles and Malik, 1999). Data expressed as median cell brightness or number of particles per cell were consistent within each treatment.

Colocalization of gp60 and FM 1-43

Confluent BLMVEC on coverslips were incubated for 15 min at 37°C in a mixture of 5 μg/ml FM 1-43 and 5 μg/ml Cy3-conjugated anti-gp60 Ab in HBSS plus 10 mg/ml BSA to colabel cytosolic vesicles. Cells were washed quickly three times with ice-cold HBSS containing 10 mg/ml albumin to remove external FM 1-43 and three times for 5 min each with ice-cold pH 5.0 buffer (0.1 M NaCl plus 0.05 M sodium acetate) to remove Cy3-labeled anti-gp60 Ab attached to cell-surface gp60. The cells were warmed to 37°C for 5 or 45 min to allow the colabeled vesicles to migrate. Cells were viewed by laser scanning confocal microscopy (laser scanning microscope [LSM] 410 and 510; Carl Zeiss) in sequential optical sections. The section plane was advanced in 0.1-μm increments through the cell from the apical to the basolateral side. At each optical plane, the specimen was scanned at 488 nm to excite FM 1-43 and then at 568 nm to excite Cy3 (argon/krypton laser). FM 1-43 (green) and Cy3 (red) images were overlaid and analyzed for coincident red and green pixels (thus the colocalized fluorescence was in yellow).

Localization of gp60, $G_{\alpha i}$, and Caveolin-1

Cellular localization of $G_{\alpha i}$, gp60, and caveolin-1 in the plasma membrane and plasmalemmal vesicles of endothelial cells exposed to albumin or gp60 cross-linking (described above) was determined by immunocytochemical labeling and laser scanning confocal microscopy (Zeiss LSM 210 and 510). BLMVEC were serum-deprived for 24 h, washed three times with Hepes-buffered HBSS or phenol red-free DME, and exposed to 6 mg/ml BSA in the presence or absence of 50 μg/ml Alexa 488–conjugated BSA and/or 3.5 μg/ml cy3-anti-gp60 Ab for up to 30 min. Cells were either washed three times with HBSS and imaged live, or fixed with 4% paraformaldehyde in HBSS and blocked for 30 min in HBSS containing 5% goat serum, 0.1% Triton X-100, and 0.01% NaN_3. Primary Ab labeling was performed overnight at 4°C with anti–caveolin-1 mAb (1 μg/ml), polyclonal anti-$G_{\alpha i}$ Ab (1:100 dilution), or 20 μg/ml anti-gp60 IgG. Coverslips were washed three times for 10 min in HBSS, blocked for 30 min with 5% goat serum, and incubated for 2 h at room temperature with fluorescently labeled goat anti–rabbit and goat anti–mouse Ab. In some cases, 4′,6-diamidino-2-phenylindole, dihydrochloride (DAPI; 1 μg/ml) was added to visualize the nucleus. Confocal microscopy was performed using 364-, 488-, and 568-nm excitation laser lines to detect DAPI (BP385-470 nm emission), FITC/Alexa 488 (BP505-550 emission), and rhodamine/Alexa 568 fluorescence (LP585 emission) in optical sections <1 μm in thickness (pinhole set to achieve 1 Airy unit).

Pertussis Toxin Treatment

Confluent BLMVEC were incubated in DME containing 100 ng/ml pertussis toxin for 6 h at 37°C. Control cells were incubated in toxin-free medium for 6 h before labeling with the styryl dye.

Filipin Treatment

Confluent BLMVEC were serum-deprived for 24 h and pretreated with 50 nM filipin (25 ng/ml) for 30 min at 37°C. Control cells were incubated with serum- and phenol red–free DME containing vehicle DMSO (0.005% DMSO).

Plasmid Transfection Studies

Expression of $G_{\alpha i}$ minigene, wt-caveolin-1, and dn-Src. BLMVEC were grown to 50% confluence in 60-mm-diam plates and transfected using Ef-

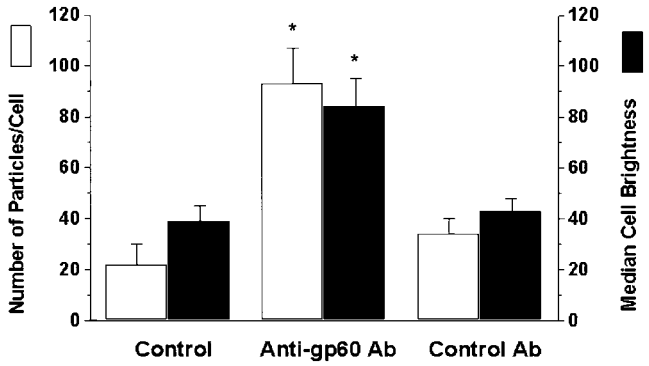

Figure 2. Activation of gp60 using cross-linking Ab increases vesicle formation in endothelial cells. BPMVEC were incubated with either anti-gp60 Ab (plus secondary Ab) or control Ab (preimmune IgG; 5 μg/ml) for 30 min at 4°C. Cells were incubated at 37°C for 15 min with 5 μg/ml FM 1-43 plus 10 mg/ml BSA. Median brightness values of cells and the number of fluorescent particles per cell were determined after three washes with buffer. The asterisk indicates increased particle density and median cell brightness ($P < 0.05$) from corresponding control values.

fectene (QIAGEN Inc.) according to manufacturer's protocol. Plasmid DNA–Effectene complexes containing either 0.25 μg/ml vector alone, wt-caveolin-1, wt-*Src*, dn-*Src*, dn-PKCα, or $G_{\alpha i}$-, $G_{\alpha q}$-, or G_{α}-random sequence minigene constructs were incubated with 0.25 μg/ml GFP (GIBCO BRL) in DME containing 10% FBS. The transfection mixture was removed after 6 h and fresh media containing 10% FBS was applied. At 24 h after transfection, cells were trypsinized and transferred to either multiwell Lab-tek chambers for styryl pyridinium dye uptake studies, to 35-mm-diam wells for obtaining cell lysates, or to 12 mm-diam No. 1 glass coverslips for immunostaining. Cells were allowed to grow for an additional 24 h, and then used for experiments (48 h after transfection). Transfection efficiency was >30%.

Coimmunoprecipitation of Caveolin-1 and gp60

Confluent BLMVEC in 60-mm-diam culture dishes were kept in serum-free medium overnight and metabolically labeled with 200 μCi/ml ^{32}P-orthophosphate for 4 h. Cells were stimulated for 20 min with 6 mg/ml BSA and lysed (30 min at 4°C in 50 mM Tris-HCl, pH 7.5, containing 150 mM NaCl, 1 mM EDTA, 0.25% sodium deoxycholate, 1.0% NP-40, 0.1% SDS, 1 mM Na_3VO_4, 1 mM NaF, 2 μg/ml leupeptin, 2 μg/ml pepstatin A, 2 μg/ml aprotinin, and 44 μg/ml PMSF). Insoluble material was removed by centrifugation (13,000 *g* for 15 min) before overnight immunoprecipitation with preimmune IgG (10 μg/ml), anti-gp60 Ab (10 μg/ml), or polyclonal anti–caveolin-1 Ab (1 μg/ml) at 4°C. Protein A or G agarose beads were added to each sample and incubated for 1 h at 4°C. Immunoprecipi-

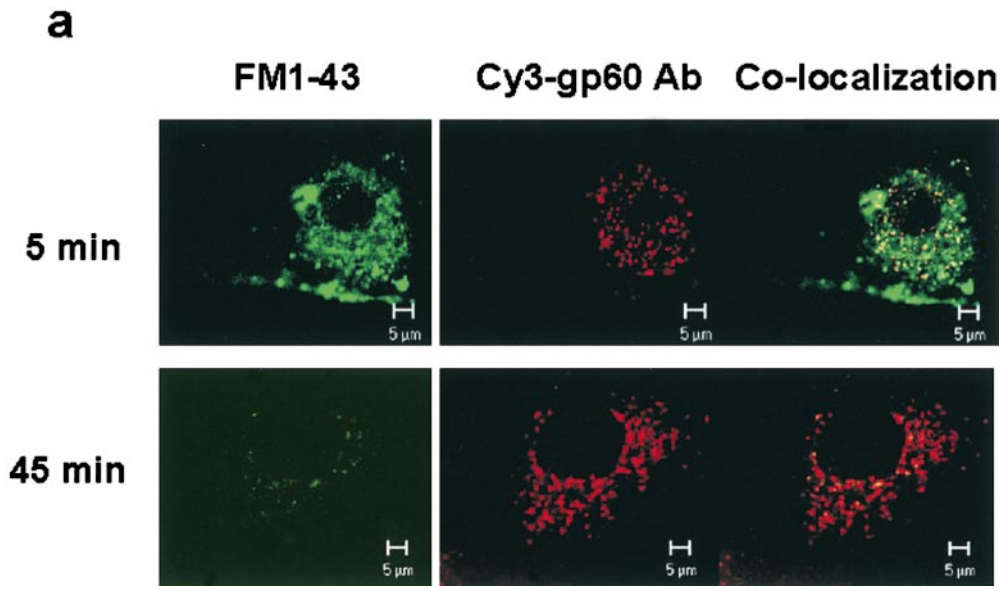

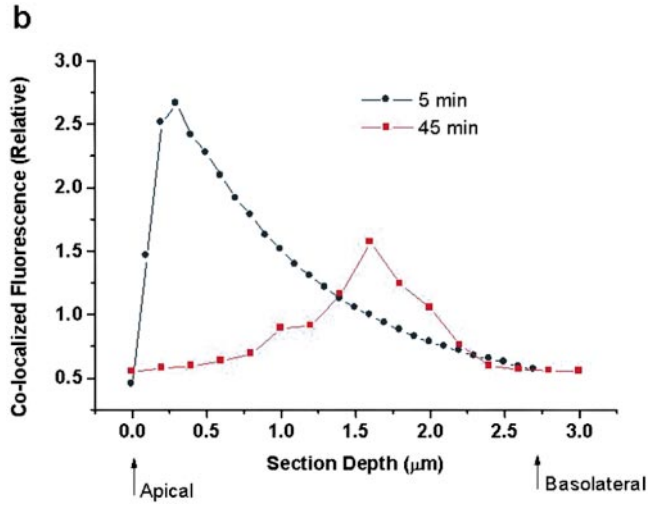

Figure 3. Colocalization and migration of gp60 and plasmalemma-derived vesicles. (a) Cy3-labeled anti-gp60 Ab was used to fluorescently tag gp60 in BLMVEC incubated in 10 mg/ml BSA. Endosomes were labeled at the same time with 5 μg/ml FM 1-43 to show colocalization of vesicles with gp60. After coincubation with both probes for the indicated times, cell-surface fluorescence was removed by extensive rinsing with pH 5.0 buffer at 4°C. Top row shows confocal images (63× objective), near the luminal cell surface, of early (5 min) intracellular fluorescence because of vesicle marker FM 1-43 (green, left), cy3-labeled anti-gp60 Ab (red, middle), and colocalization image (yellow, right). Bottom row shows albumin cell surface after exocytosis. Note the relative absence of colocalization at 45 min. (b) Plot of migration of gp60-containing vesicles in an endothelial cell. Plot gives relative colocalized fluorescence intensity versus depth of the optical section through the endothelial cell. Peak fluorescent intensity occurred near the luminal cell surface at 5 min after co-labeling, whereas the peak is shifted towards the basolateral surface at 45 min. The peak colocalized fluorescence intensity decreased at 45 min compared with 5 min because of exocytosis of FM 1-43 and dilution of its fluorescence in extracellular fluid. Results are representative of five experiments.

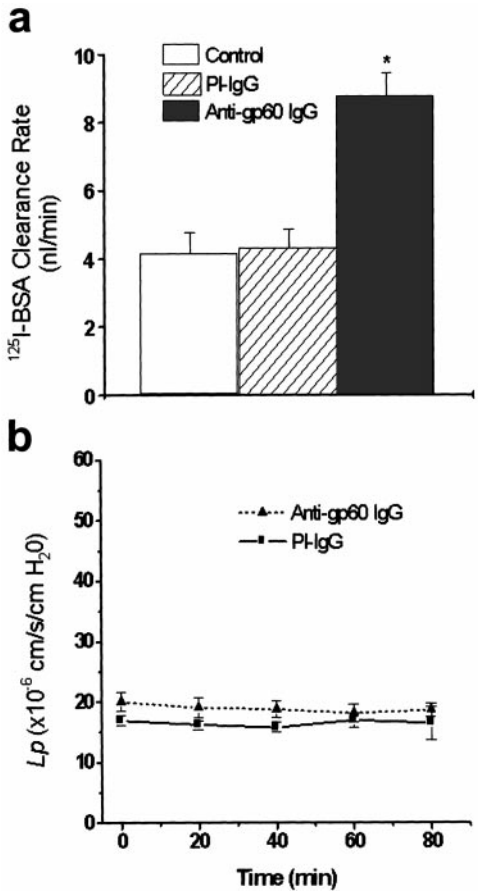

Figure 4. Gp60 activation increases transendothelial flux of ^{125}I-albumin without increasing barrier hydraulic conductivity. (a) BLMVEC monolayers on filters were washed twice with Hepes-DME and incubated with either anti-gp60 Ab or preimmune (PI) IgG (10 μg/ml) for 30 min at 22°C, followed by treatment with 10 μg/ml goat anti–rabbit secondary Ab for 30 min. Monolayers were used for transendothelial ^{125}I-albumin permeability measurements at 37°C. Both luminal and albuminal compartments contained 30 mg/ml of unlabeled albumin. Asterisk indicates the difference from control ($P < 0.001$). (b) Lack of effect of gp60 cross-linking on endothelial monolayer hydraulic conductivity (L_p). A system consisting of BLMVEC cultured on filters using the two compartment system was used to measure L_p (Qiao et al., 1993); medium albumin concentration was 5 mg/ml. Monolayers were washed and incubated with either anti-gp60 Ab (to induce gp60 cross-linking) or preimmune IgG (10 μg/ml) for 10 min, followed by secondary Ab treatment for 5 min. Values are the mean ± SEM ($n = 5$).

tates were gently washed three times with 150 mM Tris-HCl buffer containing 0.05% Triton X-100, 1 mM Na_3VO_4, 1 mM NaF, 2 μg/ml leupeptin, 2 μg/ml pepstatin A, 2 μg/ml aprotinin, and 44 μg/ml PMSF. Immunoprecipitated proteins were resolved on SDS-PAGE, transferred to Duralose membrane, and visualized by autoradiography. Protein bands were identified by reprobing with either anti-gp60 Ab or anti–caveolin-1 Ab.

Western Blot Analysis

BLMVEC lysates (10 μg protein was loaded per lane) were resolved by SDS-PAGE on a 12% separating gel under reducing conditions and transferred to Duralose membrane. Membranes were blocked with (5% dry milk in 10 mM Tris-HCl, pH 7.5, 150 mM NaCl, 0.05% Tween-20) for 2 h at 22°C. Membranes were incubated with a 1:3,000 dilution of polyclonal anti–caveolin-1 Ab or 0.4 μg/ml anti-$G_{\alpha i}$ or $G_{\alpha q}$ Ab at 22°C for 3 h. After washes, membranes were incubated at 22°C with HRP-conjugated goat anti–rabbit Ab. After incubation, membranes were washed twice, and protein bands were localized by incubating with enhanced chemiluminescence reagent (Pierce Chemical Co.).

Statistical Analysis

Statistical comparisons were made using the *t* test with the significance level set at $P < 0.05$.

Results

Activation of gp60 Induces Plasmalemmal Vesicle Formation

The cellular distribution of gp60 was determined after incubating confluent endothelial cells for 30 min with Cy3-conjugated anti-gp60 Ab. We observed punctate distribution of fluorescence after incubation of the probe at 37°C, followed by cold (4°C) wash buffer to remove the cell surface–bound Cy3 probe (Fig. 1 a). To visualize internalized gp60, cell-surface fluorescence was removed by an acid wash. The resultant image showed that gp60 was internalized during the incubation period (Fig. 1 b). Reduction of the temperature to 4°C followed by a low pH wash prevented the gp60 internalization (Fig. 1 c).

Endothelial cell monolayers were incubated with styryl pyridinium dye, FM 1-43 (5 μg/ml), for 15 min at 37°C, and then rinsed with dye-free buffer to visualize plasmalemma-derived endocytic vesicles. Endothelial cells incubated in FM 1-43 exhibited the punctate distribution of fluorescence characteristic of vesicles (Fig. 1 d). Vesicle formation was inhibited when cells were kept at 4°C during the dye loading period (Fig. 1 e).

To determine the effects of gp60 cross-linking on vesicle formation, BLMVEC were incubated with either anti-gp60 Ab or preimmune IgG (control Ab) for 30 min at 4°C followed by anti-rabbit secondary Ab for 30 min at 4°C. Cells were exposed to FM 1-43 for 15 min at 37°C, membrane-bound dye was washed, and intracellular FM 1-43 fluorescence was quantified as median brightness of cells and the number of fluorescent particles per cell. The gp60 cross-linking produced 2.0–3.8-fold increases in cell fluorescence by either measure compared with controls (Fig. 2).

Activation of gp60 Induces Transcellular Migration of Plasmalemma-derived Vesicles

To determine the fate of gp60 and of vesicles formed by gp60 activation, FM 1-43–labeled vesicles were colocalized with the Cy3-conjugated anti-gp60 Ab. Cells were washed with acid buffer to detach Cy3-anti-gp60 Ab from the cell surface before imaging. Confocal images of each fluorescent probe were obtained at 0.1-μm z-axis step increments from the apical to basolateral cell membrane. Colocalization was determined by merging red (Cy3 fluorescence) and green images (Fig. 3 a; FM 1-43 fluorescence). Although FM 1-43 labels all plasmalemmal-derived vesicles, a fraction of these vesicles were colocalized (yellow) with the fluorescently labeled gp60 Ab.

To follow the migration of plasmalemma-derived vesicles, endothelial cells were colabeled with fluorescent anti-gp60 Ab and FM 1-43 for 15 min at 37°C, washed (4°C), and rewarmed (37°C) for either 5 or 45 min to activate the ves-

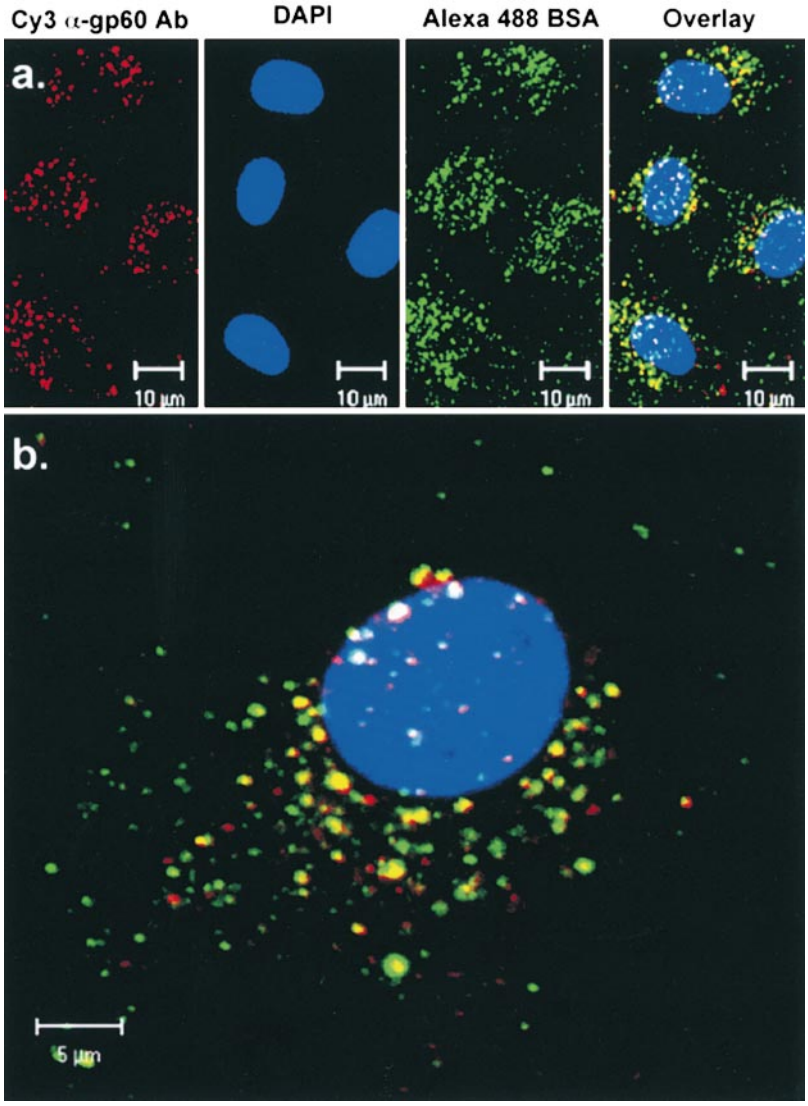

Figure 5. Colocalization of gp60 with albumin. Confocal images of BLMVEC grown to confluence on gelatin-coated glass coverslips showing fluorescent staining of gp60, DAPI, and Alexa 488-albumin. (a) Single section (<1.0 μm thick; four frame average) near the apical membrane surface showing gp60 (red), DAPI (blue), albumin (green), and the overlay of gp60, albumin, and DAPI immunostaining in BLMVEC. (b) Merged images of gp60, DAPI, and albumin in confocal z-axis optical sections (0.2-μm step size; two frame averages) through a single BLMVEC. Projection image (22 sections stacked) en face (b) show the distribution of gp60 and albumin in the cell.

icle migration. At 5 min after colabeling, the vesicles that formed during the dye incubation period were located in the cytosol near the apical plasmalemma; i.e., in upper one-third of each cell (Fig. 3 a, top row). At 45 min after colabeling, the vesicles containing gp60 and endocytic marker dye had migrated to the lower half of the cell near the basolateral plasmalemma (Fig. 3 a, bottom row).

Fig. 3 b shows the colocalization of fluorescence in different optical section depths of the cell at either 5 or 45 min after gp60 activation. At 5 min after gp60 activation, the peak colocalized fluorescence (i.e., the gp60-activated vesicles) was observed <0.5 μm from the apical surface. At 45 min, the peak colocalized fluorescence was shifted toward the basolateral cell surface (i.e., at a section depth of 1.5 μm). Because of the release of styryl dye into the basolateral extracellular compartment, the immunofluorescence intensity of the 45-min peak was markedly diminished, such that residual immunofluorescence primarily reflected the persistence of gp60 antigen in the basolateral aspect of the cell.

Effects of gp60 Activation on Transendothelial ^{125}I-Albumin Flux and Endothelial Hydraulic Conductivity

We measured transendothelial flux of tracer ^{125}I-albumin and hydraulic conductivity in confluent BLMVEC monolayers grown on polycarbonate filters to determine gp60-activated transendothelial albumin permeability and its relationship to liquid permeability. Cross-linking of gp60 at 37°C using 10 μg/ml anti-gp60 Ab plus secondary Ab increased transendothelial ^{125}I-albumin permeability by twofold (Fig. 4 a). However, the increased ^{125}I-albumin permeability was dissociated from endothelial monolayer hydraulic conductivity (L_p; Fig. 4 b). As gp60 activation increased transendothelial albumin permeability without increasing water permeability, the results indicate increased albumin flux through transcellular pathways.

Colocalization of gp60 and Albumin in Plasmalemma-derived Vesicles

To determine the pattern of localization of gp60 and albu-

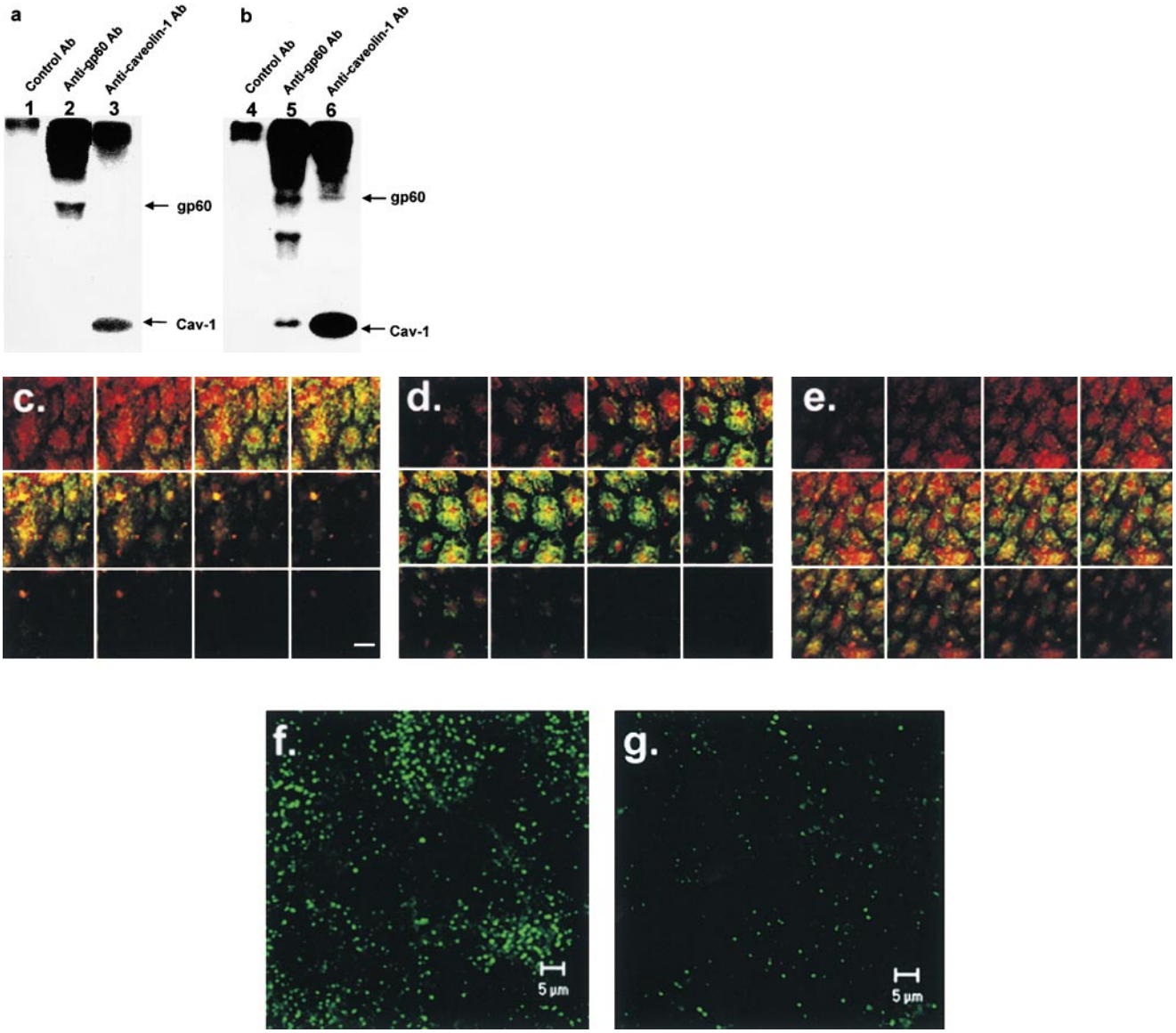

Figure 6. Coimmunoprecipitation and migration of caveolin-1 and gp60. BLMVEC were grown to confluence, serum-deprived overnight, and metabolically labeled for 4 h with 200 μCi/ml ^{32}P-orthophosphate. Cells were either stimulated for 20 min with 6 mg/ml BSA (b) or not stimulated with BSA (a) and lysed. Total cell lysate was immunoprecipitated with preimmune rabbit IgG (lanes 1 and 4), rabbit anti-gp60 IgG (lanes 2 and 5), or rabbit anti–caveolin-1 IgG (lanes 3 and 6), separated by SDS-PAGE, transferred to a nitrocellulose membrane, and visualized by autoradiography. As shown in lane 4 (b), the cell lysate that immunoprecipitated with the anti-gp60 Ab also contained a 22-kD protein, which migrated similarly to that immunoprecipitated with anti–caveolin-1 Ab (b, lane 6). (b) Lane 6 shows that the cell lysate that immunoprecipitated with anti–caveolin-1 Ab also pulled down a protein similar to that immunoprecipitated with the anti-gp60 Ab (b, lane 5). Control Ab did not immunoprecipitate either ^{32}P-labeled protein. In the absence of albumin stimulation, gp60 was not coimmunoprecipitated with the anti–caveolin-1 Ab (a, lane 2 and 3). Results are representative of three experiments. (c–e) Merged images of gp60 (red) and caveolin-1 (green) immunostaining of BLMVEC monolayers after albumin exposure for 0 (c), 3 (d), or 30 min (e). Gp60 and caveolin-1 staining appeared near the apical surface in the absence of added albumin (c, top panel). With the addition of albumin, gp60 migrated towards the basolateral aspect of the cell monolayer (d, at 3 min, middle panel, and e, at 30 min, bottom panel of images). The green fluorescence did not redistribute with time to the same extent as gp60. (f and g) Effects of filipin on fluorescent albumin uptake. BLMVEC were pretreated with vehicle (f, control) or 50 nM filipin (g) for 30 min at 37°C, and then incubated with medium containing 5 mg/ml BSA and 50 μg/ml Alexa 488 albumin for 30 min at 37°C. The cells were washed and imaged for albumin internalization. Results are representative of five experiments. Bar, 20 μm.

min after activation of gp60, we evaluated immunostaining of cells after a 30 min incubation (37°C) with Cy3-anti-gp60 Ab and Alexa 488 BSA in phenol red–free DME containing 5 mg/ml albumin. Fig. 5 a shows the punctate fluorescent structures containing gp60 Ab (red), DAPI staining of the nucleus (blue), and fluorescently labeled albumin (green) near the apical membrane of BLMVEC. An overlay image (Fig. 5 a, far right) of the three probes shows a high degree of gp60 and albumin colocalization (in yellow). A projection image of BLMVEC gp60, DAPI, and

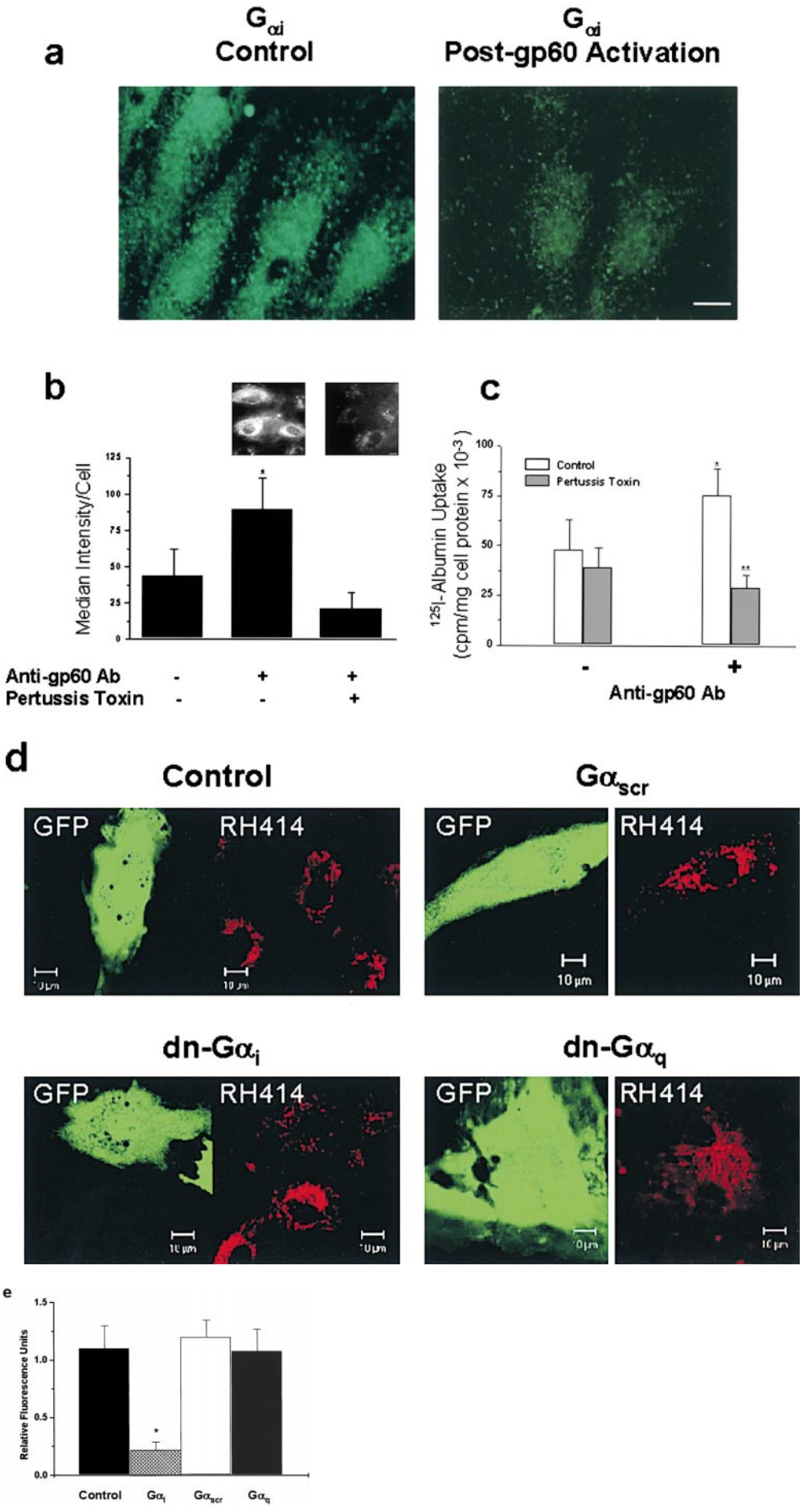

Figure 7. Role of G_i signaling in gp60-induced vesicle formation. (a) Cell-surface $G_{\alpha i}$ immunostaining decreases after gp60 activation. BLMVEC exposed to vehicle (left) or anti-gp60 Ab (right) for 10 min at 37°C were labeled with polyclonal anti-$G_{\alpha i}$ Ab plus Alexa 488–conjugated goat anti–rabbit secondary Ab. Confocal images (eight frame average, <1.0-µm thick optical sections near the apical plasma membrane) were acquired with a Zeiss LSM 210. (b) Pertussis toxin inhibits gp60-activated vesicle formation. BLMVEC were preincubated for 6 h at 37°C in medium containing 100 ng/ml pertussis toxin. At end of the preincubation period, endocytosis was stimulated by 30 min of incubation in 5 µg/ml anti-gp60 Ab to cross-link gp60. FM 1-43 (5 µg/ml) was added to cells during the final 15 min of Ab incubation; excess styryl dye was washed away with three changes of ice-cold buffer. Control cells received no toxin during 6-h preincubation period. Median cellular fluorescence intensity is shown. Pertussis toxin blocked FM 1-43 endocytic marker dye uptake that was induced by the activation of gp60 with anti-gp60 Ab (gp60 cross-linking). The asterisk indicates an increase ($P < 0.05$) of median fluorescence intensity because of gp60 cross-linking (in the absence of pertussis toxin). (b, inset) Fluorescent images of cells: (left) no pertussis toxin; (right) pertussis toxin treatment. Results are representative of three experiments. (c) Pertussis toxin (100 ng/ml for 6 h) inhibits ^{125}I-albumin uptake in endothelial cells induced by gp60 cross-linking. Cells were incubated in ^{125}I-labeled tracer albumin for 25 min after gp60 cross-linking, washed three times in pH 2.5 buffer, lysed, and counted for ^{125}I-labeled albumin. Bars indicate SD ($n = 3$). The single asterisk indicates a difference from no anti-gp60 Ab (−) control group ($P < 0.05$); and the double asterisk indicates a decrease relative to the anti-gp60 Ab–activated

albumin fluorescent staining is shown in Fig. 5 b. The en face (x-y) view of stacked z-plane images (22 sections) showed marked colocalization of gp60 Ab and albumin in the same endocytic vesicles (Fig. 5 b).

Gp60 and Caveolin-1 Interaction

We metabolically labeled serum-deprived BLMVEC with ^{32}P-orthophosphate for 4 h, stimulated with or without 6 mg/ml albumin for 20 min, and prepared the cell lysates for immunoprecipitation to study caveolin-1 and gp60 interactions (see Materials and Methods). Incubation of the cell lysate with control Ab failed to precipitate either gp60 or caveolin-1 (Fig. 6, a and b, lanes 1 and 4). In the absence of albumin, anti-gp60 Ab or anti–caveolin-1 Ab immunoprecipitates revealed 60- and 22-kD proteins (Fig. 6 a, lane 2 and 3), which corresponded to gp60 and caveolin-1, respectively. However, in the case of albumin stimulation, anti-gp60 Ab immunoprecipitated 60-, 36-, and 22-kD proteins (Fig. 6 b, lane 5). The 60- and 22-kD bands were identified as gp60 and caveolin-1, respectively, by Western blotting (not shown). The 36-kD band may be CD36, the low density lipoprotein receptor (Huang et al., 1991; Lisanti et al., 1994; Tiruppathi et al., 1997). In addition, anti–caveolin-1 Ab precipitated caveolin-1 as well as gp60 in the albumin-stimulated cells (Fig. 6 b, lane 6). Thus, the physical association of gp60 with caveolin-1 in endothelial cells is facilitated by the activation of gp60 with albumin.

Serum-deprived BLMVEC were stimulated with albumin for 0, 3, or 30 min, and were fixed and stained with anti-gp60 and caveolin-1 Abs to address whether gp60 and caveolin-1 immunostaining comigrated from the apical to basolateral surfaces as a function of albumin exposure. In the absence of albumin, gp60 (red) and caveolin-1 (green) immunostaining, which showed a marked overlap (in yellow), appeared near the apical surface of BLMVEC monolayers (Fig. 6 c), as seen in the z-axis optical sections (top left, apical surface; bottom right, basolateral surface). Exposing cells to 6 mg/ml BSA for 3 min (Fig. 6 d) or 30 min (Fig. 6 e) to activate gp60 induced the internalization and basolateral migration of gp60. The green fluorescence, which marked caveolin-1, did not redistribute towards the basolateral membrane to the same extent as gp60. In control experiments, nonspecific immunofluorescence observed in the presence of preimmune rabbit IgG, control mouse IgG, or with secondary antibodies alone was minimal; it did not show a pattern of colocalization and also did not change after the exposure of endothelial cell monolayers to albumin.

BLMVEC were treated with filipin to determine whether disruption of caveolae influenced albumin uptake induced by gp60. BLMVEC were incubated in the presence or absence of 50 nM filipin for 30 min at 37°C and incubated with anti-gp60 Ab for 30 min at 4°C to cross-link gp60. Cells were incubated with Alexa 488-BSA for 30 min in media containing 5 mg/ml of unlabeled BSA and acid-washed to remove extracellular label. As shown in Fig. 6 g, filipin prevented the formation of vesicles as compared with control cells (Fig. 6 f).

G_i Transduces gp60-activated Vesicle Formation

We used three approaches to address the role of G_i in the mechanism of gp60-induced vesicle formation and trafficking: (1) pertussis toxin, which prevents activation of G_i/G_0 by ADP ribosylation (Hepler and Gilman, 1992); (2) transfection of the dn construct encoding the 11–amino acid carboxyl-terminal peptide sequence of $G_{\alpha i1/2}$,which competes for $G_{\alpha i}$–receptor interactions (Gilchrist et al., 1998); and (3) $G_{\alpha i}$ immunostaining.

In control BLMVEC, $G_{\alpha i}$ was localized in the apical membrane (Fig. 7 a, left). Cross-linking of gp60 for 10 min resulted in a decreased apical membrane–associated $G_{\alpha i}$ immunostaining (Fig. 7 a, right). Pretreatment of endothelial monolayers with the pertussis toxin prevented both FM 1-43 and ^{125}I-albumin endocytosis induced by gp60 (Fig. 7, b and c). In addition, the expression of $G_{\alpha i}$ carboxyl-terminal peptide (dn-$G_{\alpha i}$) in BLMVEC also prevented the gp60-activated vesicle formation as determined by RH 414 uptake in green fluorescent protein (GFP)–positive endothelial cells (Fig. 7, d and e). In control experiments, endothelial cells transfected with the $G_{\alpha q}$ minigene (dn-$G_{\alpha q}$) or control minigene encoding a randomized sequence of $G_{\alpha i}$ carboxyl terminus ($G_{\alpha\text{-scr}}$; Fig. 7, d and e) showed the characteristic activation of endocytosis secondary to gp60 stimulation.

Expression of Caveolin-1 and dn-Src Inhibit Vesicle Formation

We studied the effects of overexpression of wt-caveolin-1 since caveolin-1 can bind to $G_{\alpha i}$ (Li et al., 1995) and, thus, may functionally inactivate endogenous $G_{\alpha i}$. Since caveolin-1 and gp60 are phosphorylated by *Src* family kinases after gp60 activation (Tiruppathi et al., 1997), we also studied the role of *Src* by inducing the expression of dn-*Src*. Whole cell lysates from BLMVEC transfected with vector alone (Mock), wt-caveolin-1 (wt-Cav-1), or dn-*Src* were immunoprecipitated with anti–caveolin-1 Ab, separated by SDS-PAGE, and blotted with Abs against caveolin-1, $G_{\alpha i}$, and $G_{\alpha q}$ (Fig. 8). The resulting blots showed a twofold increase in expression of caveolin-1 in cells transfected with wt-caveolin-1 (lane 2) compared with mock-

(+) group ($P < 0.05$). (d and e) Expression of $G_{\alpha i}$ carboxyl-terminal peptide in endothelial cells inhibits gp60-activated endocytosis. (d) BLMVEC were cotransfected with GFP in pcDNA3.1 and a pcDNA3.1 expression vector containing the minigene construct encoding an 11–amino acid carboxyl-terminal sequence of the guanine nucleotide binding protein $G_{\alpha i}$ (dn-$G_{\alpha i}$), $G_{\alpha q}$, (dn-$G_{\alpha q}$), or a randomized sequence ($G_{\alpha\text{-scr}}$). The cells were serum-deprived for 24 h and incubated for 15 min with 6 mg/ml BSA and 5 μg/ml RH 414. Images of RH 414 dye uptake were acquired in transfected cells (GFP-positive) by confocal microscopy. (e) Summary of RH 414 fluorescence intensity in G-protein minigene–transfected cells. Expression of $G_{\alpha i}$-carboxyl-terminal peptide inhibited gp60-activated endocytosis in BLMVEC, whereas BLMVEC expressing $G_{\alpha q}$ peptide or G_{α}-randomized sequence peptide showed the characteristic endocytic response secondary to gp60 activation. The asterisk indicates decrease from corresponding control values (cells transfected with dn-$G_{\alpha q}$ or G_{α}-randomized sequence peptide; $P < 0.05$). Bar: (a) 10 μm; (b) 2 μm.

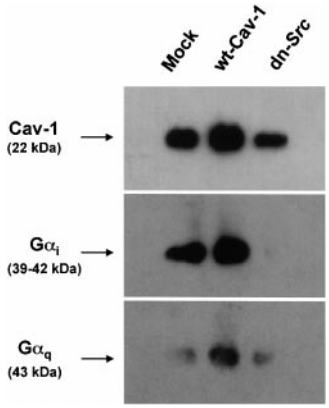

Figure 8. Effects of caveolin-1 overexpression and dominant negative *Src* (dn-*Src*) expression on the association of $G_{\alpha i}$ and $G_{\alpha q}$ with caveolin-1. BLMVEC transfected with pcDNA3.1 alone (Mock); and wt-caveolin-1 (cav-1) or dn-*Src* was grown to confluence (48 h posttransfection). Cells were washed and lysed (see details in Materials and Methods), and the lysate was immunoprecipitated using 2.5 μg/ml anti–caveolin-1 Ab. Precipitated proteins were separated by SDS-PAGE and transferred to the Duralose membrane. The membrane was blotted with anti–caveolin-1 Ab (top), anti-$G_{\alpha i}$ Ab (middle), and anti-$G_{\alpha q}$ Ab (bottom). Representative data from three experiments are shown.

transfected cells (lane 1). Caveolin-1 overexpression augmented the association of caveolin-1 with both $G_{\alpha i}$ and $G_{\alpha q}$ (lane 2), indicating the sequestration of G-proteins with the expressed caveolin-1. Expression of dn-*Src* decreased the amount of caveolin-1 (Fig. 8, lane 3, top) and abolished association of caveolin-1 with $G_{\alpha i}$ (Fig. 8, lane 3, middle), whereas it had no effect on caveolin-1 association with $G_{\alpha q}$ (Fig. 8, lane 3, bottom panel). Thus, the dissociation of $G_{\alpha i}$ from caveolin-1 induced by dn-*Src* suggests an important role of *Src* in regulating the integrity of the caveolin-1/$G_{\alpha i}$ signaling complex.

To determine the effects of caveolin-1 overexpression and dn-*Src* expression on gp60-activated vesicle formation, GFP was co-expressed with wt-caveolin-1 or dn-*Src* in BLMVEC, and styryl dye uptake was measured in the GFP-positive cells. Images of GFP-positive cells in the left panels (Fig. 9, a, c, and e) are shown with images of the same field of RH 414 uptake in the right panels (Fig. 9, b, d, and f). In cells expressing the empty vector (Fig. 9 a), we observed gp60-activated RH 414 dye uptake (Fig. 9 b). However, overexpression of wt-caveolin-1 (Fig. 9 c) or expression of dn-*Src* (Fig. 9 e) prevented vesicle formation (Fig. 9, d and f) in the GFP-positive cells, but not in the nontransfected cells (ntf). As a control for dn-*Src*, wt-*Src* and dn-PKCα were co-expressed with GFP in BLMVEC. In these control experiments, we observed the characteristic activation of endocytosis secondary to gp60 activation (Fig. 9, g–h). Thus, the results show that caveolin-1 overexpression and dn-*Src* expression abolished gp60-activated vesicle formation in endothelial cells.

Discussion

Serum albumin is critical for the maintenance of the normal oncotic pressure gradient across microvessels and for stability of the endothelial barrier (Michel and Curry, 1999). The endothelial cell monolayer has the capacity to regulate the directed movement of albumin between its luminal and albumin membrane surface. Transcytosis involves albumin uptake from the vascular space by endocytosis, the vectorial transfer of vesicles from the apical to the basolateral membrane, and the release of albumin by exocytosis into the subendothelial space. Transcytosis may be physiologically important in regulating the transendothelial albumin concentration gradient and transport of albumin-bound ligands such as hormones, nonesterified fatty acids, and ions.

The endothelial cell-surface glycoprotein gp60, an albumin-binding protein, has been invoked in the mechanism of albumin transcytosis (Schnitzer et al., 1988; Ghinea et al., 1989; Schnitzer, 1992; Schnitzer and Oh, 1994; Tiruppathi et al., 1996, 1997). The present study provides new information on the signal transduction pathways activated by gp60 that induce the formation of vesicles and the targeted migration of vesicles to the basolateral membrane. We showed that upon gp60 activation, gp60 becomes colocalized with albumin and it interacts with caveolin-1. Albumin, the gp60 ligand, did not induce the formation of plasmalemmal-derived vesicles in brain microvessel endothelial cells that lacked gp60 (Minshall et al., data not shown). Vesicle formation, which was activated by gp60, required the heterotrimeric G protein G_i, since treatment of cells with pertussis toxin and expression of an antagonist peptide, which uncouples $G_{\alpha i}$ from its receptor binding site (Gilchrist et al., 1998), prevented the budding of vesicles and albumin endocytosis. Overexpression of wt-caveolin-1, which was shown to sequester $G_{\alpha i}$, and expression of dn-*Src* also prevented the gp60-induced vesicle formation by interfering with the G_i signaling pathway.

The present study demonstrates an important role of gp60 in stimulating endocytosis and the directed migration of vesicles in endothelial cells. Analysis of serial confocal sections showed the apical-to-basolateral migration of vesicles activated by gp60 in live endothelial cells, which is suggestive of a transcytotic process. We showed that vesicular markers (FM 1-43 and RH 414) were taken up in the apical membrane–derived, gp60-positive vesicles, and that the destaining of vesicular markers occurred at the basolateral endothelial cell surface. Interestingly, gp60 remained localized in the basolateral vesicles after the release of styryl dye, suggesting that gp60 has the potential to recycle to the apical membrane and to reactivate endocytosis. In addition, we showed that gp60 activation (with cross-linking Ab) also increased ^{125}I-labeled albumin clearance across endothelial monolayers and the transcellular migration of styryl pyridinium dye-filled vesicles. Thus, the activation of gp60-induced transcellular membrane traffic was associated with increased transendothelial albumin permeability. However, gp60 activation did not change the endothelial barrier L_P, suggesting that the interendothelial junctional or paracellular permeability pathway did not increase when albumin transport was stimulated by gp60. These physiological experiments provide further proof that increased albumin permeability after gp60 activation occurred via a transcellular or nonhydraulic permeability pathway.

Caveolae, the nonclathrin-coated pits that are abundant in vascular endothelial cells, have been implicated in the mechanism of endocytosis (Lisanti et al., 1994; Anderson, 1998) and transcellular permeability (Milici et al., 1987; Schnitzer et al., 1994; Tiruppathi et al., 1997). We showed that gp60 and caveolin-1, the caveolar structural protein

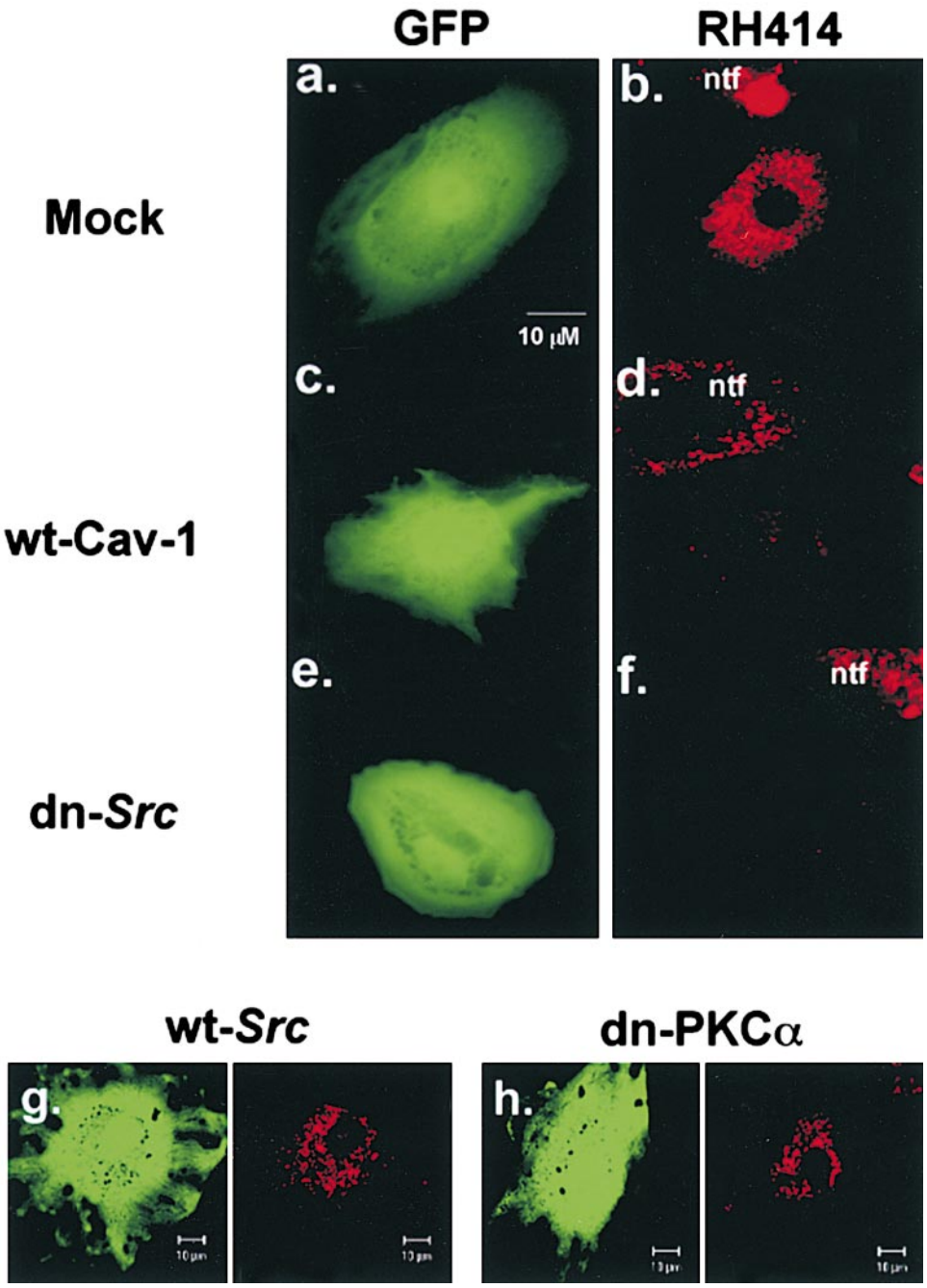

Figure 9. Effects of caveolin-1 overexpression and dominant negative *Src* (dn-*Src*) expression on gp60-induced vesicle formation. BLMVEC cotransfected with GFP and either 0.25 μg/ml vector alone, wt-caveolin-1, or dn-*Src* were plated in 4-well Lab-tek chambers and, at 48 h after transfection, were assayed for RH 414 uptake induced by albumin. Cells were incubated with 5 μg/ml RH 414 for 15 min at 37°C, rinsed three times in HBSS (4°C), and whole cell fluorescent images of RH 414 were acquired in GFP-positive cells. (a and b) BLMVEC transfected with vector alone; (c and d) cell transfected with wild type caveolin-1; (e and f) cell transfected with dn-*Src*. (a, c, and e) Fluorescein filter set showing a selection of a GFP-positive (and cotransfected) cell. (b, d, and f) Rhodamine filter set showing whole cell fluorescence of RH 414 from the same field shown in a, c, or e. Activation of gp60 failed to induce the formation of vesicles in the cells overexpressing caveolin-1 or expressing dn-*Src*. (g and h) Expression of wt-*Src* or dn-PKCα had no effect on RH 414 uptake. Results are representative of three to five experiments.

(Rothberg et al., 1992), were colocalized in endothelial cell apical plasma membrane–derived vesicles, and that they migrated in the basolateral direction after activation of gp60. However, caveolin-1 did not redistribute towards the basolateral membrane to the same extent as gp60, suggesting that gp60 translocates across the cell mainly, though not exclusively, with caveolin-1. Immunoprecipitation data showed that gp60 and caveolin-1 were physically associated after gp60 activation, which is suggestive of a critical interaction between gp60 and caveolin-1. Endocytosis of fluorescent albumin was blocked by filipin, a sterol-binding agent that dissembles the cholesterol-rich caveolae (Rothberg et al., 1990, 1992; Schnitzer et al., 1994). Taken together, these data support the concept that gp60-activated albumin endocytosis occurs by means of vesicles derived from caveolae. The budding of vesicles may be the result of dynamin-regulated fission of the caveolar plasmalemmal membrane (Oh et al., 1998).

Plasmalemmal membrane–derived vesicles have been shown to contain caveolin-1, G proteins, G protein–coupled receptors, and *Src* family tyrosine kinases (Chun et al., 1994; Li et al., 1996; Liu et al., 1996; Murphy et al., 1996; Song et al., 1997; Zacchi et al., 1998; for review see Anderson, 1998). Caveolin-1 is known to sequester caveolae-associated signaling proteins such as *Src* and G_i in their inactive form (Okamoto et al., 1998). As caveolin-1 may be involved in gp60-induced vesicle formation (Milici et al., 1987; Tiruppathi et al., 1997), we overexpressed caveolin-1

in endothelial cells and addressed the effects of this intervention on vesicle formation after gp60 activation. We observed that caveolin-1 overexpression sequestered $G_{\alpha i}$ and, importantly, it prevented gp60- activated vesicle formation. This finding is consistent with the role of caveolin-1 in binding (and thereby in sequestering) G proteins and other signaling molecules (Okamoto et al., 1998). We addressed the possible role of G_i in activating gp60-induced vesicle formation using pertussis toxin (Hepler and Gilman, 1992) and the expression of $G_{\alpha i}$ antagonist peptide (Gilchrist et al., 1998; Ellis et al., 1999). As both inhibitors prevented gp60-activated vesicle formation in endothelial cells, the results indicate that G_i plays a critical role in transducing the gp60-induced vesicle formation.

Since G_i induces the activation of downstream *Src* kinase (Luttrell et al., 1996; Igishi and Gutkind, 1998), we addressed whether *Src* kinase was also involved in the gp60-activated signaling cascade. The results indicated that the expression of dn-*Src* prevented gp60-activated vesicle formation in endothelial cells. Interestingly, dn-*Src* expression also prevented the binding of $G_{\alpha i}$ to caveolin-1. As *Src* kinase and $G_{\alpha i}$ can compete for a common binding domain on caveolin-1 (Li et al., 1996; Okamoto et al., 1998), an explanation for our finding is that binding of dn-*Src* to caveolin-1 displaced $G_{\alpha i}$ from caveolin-1. This could account for the observation that significantly less $G_{\alpha i}$ coimmunoprecipitated with caveolin-1 in the cells transfected with dn-*Src*. The data are consistent with the model that caveolin-1 serves as a scaffolding protein for G_i and *Src* family kinases, which activate the signaling machinery mediating the gp60-induced vesicular transport. *Src* family tyrosine kinases activated by receptor dimerization (Marshall, 1995) or by $\beta\gamma$ subunits upon stimulation of G-protein–coupled receptors (Luttrell et al., 1996; Igishi and Gutkind, 1998) may phosphorylate caveolin-1 (Lisanti et al., 1994; Li et al., 1996; Tiruppathi et al., 1997) and gp60 (Tiruppathi et al., 1997), and thereby signal vesicle formation and trafficking. Thus, the gp60–caveolin-1 complex could function in much the same manner as G-protein–coupled receptors that interact with $G_{\alpha i}$ and *Src*.

In summary, we have shown that G_i is required for signaling of vesicle formation in endothelial cells after gp60 activation. Overexpression of wt-caveolin-1 and expression of dn-*Src* prevented gp60-induced formation of vesicles. In each case, the role of G_i was important since caveolin-1–overexpressing cells sequestered $G_{\alpha i}$, whereas dn-*Src* expression interfered with the binding of $G_{\alpha i}$ to caveolin-1. These results indicate an important role of gp60-induced activation of the G_i-coupled *Src* kinase pathway in signaling the formation of endocytic vesicles and their directed migration to the basolateral surface of the vascular endothelial barrier.

This research was supported in part by National Institutes of Health grants T32 HL07239, HL60678, HL45638 (to A.B. Malik), and GM58531 (to C. Tiruppathi).

Submitted: 3 November 1999
Revised: 12 July 2000
Accepted: 13 July 2000

References

Anderson, R.G. 1998. The caveolae membrane system. *Annu. Rev. Biochem.* 67:199–225.

Betz, W.J., F. Mao, and G.S. Bewick. 1992. Activity-dependent staining and destaining of vertebrate motor nerve terminals. *J. Neurosci.* 12:363–375.

Bocci, V. 1964. Efficient labeling of serum proteins with ^{131}I using chloramine-T. *Int. J. Appl. Radiat. Isot.* 15:449–456.

Chun, M., U.K. Liyanage, M.P. Lisanti, and H.F. Lodish. 1994. Signal transduction of a G protein-coupled receptor in caveoli: colocalization of endothelin and its receptor with caveolin. *Proc. Natl. Acad. Sci. USA.* 91:11728–11732.

Del Vecchio, P.J., A. Siflinger-Birnboim, J.M. Shepard, R. Bizios, J.A. Cooper, and A.B. Malik. 1987. Endothelial monolayer permeability to macromolecules. *Fed. Proc.* 46:2511–2515.

Del Vecchio, P.J., A. Siflinger-Birnboim, P.N. Belloni, L.A. Holleran, H. Lum, and A.B. Malik. 1992. Culture and characterization of pulmonary microvascular endothelial cells. *In Vitro Cell. Dev. Biol.* 28A:711–715.

Ellis, C.A., A.B. Malik, H. Hamm, R. Sandoval, T. Voyno-Yasenetskaya, A. Gilchrist, and C. Tiruppathi. 1999. Thrombin induces PAR-1 gene expression in endothelial cells via activation of G_i-linked Ras/mitogen-activated protein kinase pathway. *J. Biol. Chem.* 274:13718–13727.

Forker, E.L., and B.A. Luxton. 1983. Albumin mediated transport of rose bengal by perfused rat liver. *J. Clin. Invest.* 72:1764–1771.

Garcia, J.G.N., A. Siflinger-Birnboim, R. Bizios, P.J. Del Vecchio, J.W. Fenton II, and A.B. Malik. 1986. Thrombin-induced increases in albumin transport across cultured endothelial monolayer. *J. Cell Physiol.* 128:96–104.

Ghinea, N., M. Eskenasy, M. Simionescu, and N. Simionescu. 1989. Endothelial albumin binding proteins are membrane-associated components exposed on the cell surface. *J. Biol. Chem.* 264:4755–4758.

Ghitescu, L., A. Fixman, M. Simionescu, and N. Simionescu. 1986. Specific binding sites for albumin restricted to plasmalemmal vesicles of continuous capillary endothelium: receptor mediated transcytosis. *J. Cell Biol.* 102: 1304–1311.

Gilchrist, A., M.R. Mazzoni, B. Dineen, A. Dice, J. Linden, W.R. Proctor, C.R. Lupica, T.V. Dunwiddie, and H.E. Hamm. 1998. Antagonists of the receptor-G protein interface block G_i-coupled signal transduction. *J. Biol. Chem.* 273:14912–14919.

Hepler, J.R., and A.G. Gilman. 1992. G proteins. *TIBS (Trends Biochem. Sci.).* 17:383–387.

Huang, M.M., J.B. Bolen, J.W. Barnwell, S.J. Shattil, and J.S. Brugge. 1991. Membrane glycoprotein IV (CD36) is physically associated with the Fyn, Lyn, and Yes protein-tyrosine kinases in human platelets. *Proc. Natl. Acad. Sci. USA.* 88:7844–7848.

Igishi, T., and J.S. Gutkind. 1998. Tyrosine kinases of the *Src* family participate in signaling to MAP kinase from both G_q- and G_i-coupled receptors. *Biochem. Biophys. Res. Commun.* 244:5–10.

Li, S., T. Okamoto, M. Chun, M. Sargiacomo, J.E. Casanova, S.H. Hansen, I. Nishimoto, and M.P. Lisanti. 1995. Evidence for a regulated interaction between heterotrimeric G proteins and caveolin. *J. Biol. Chem.* 270:15693–15701.

Li, S., J. Couet, and M.P. Lisanti. 1996. *Src* tyrosine kinases, G_α subunits, and H-Ras share a common membrane-anchored protein, caveolin. Caveolin binding negatively regulates the auto-activation of *Src* tyrosine kinases. *J. Biol. Chem.* 271:29182–29190.

Lisanti, M.P., P.E. Scherer, J. Vidugiriene, Z. Tang, A. Hermanowski-Vosatka, Y.H. Tu, R.F. Cook, and M. Sargiacomo. 1994. Characterization of caveolin-rich microdomains isolated from an endothelial-rich source: implications for human disease. *J. Cell Biol.* 126:111–126.

Liu, P., Y. Ying, Y.-G. Ko, and R.G.W. Anderson. 1996. Localization of platelet-derived growth factor-stimulated phosphorylation cascade to caveolae. *J. Biol. Chem.* 271:10299–10303.

Lum, H., and A.B. Malik. 1994. Regulation of vascular endothelial barrier function. *Am. J. Physiol.* 276:L223–L241.

Luttrell, L.M., B.E. Hawes, T. Van Biesen, D.K. Luttrell, T.J. Lansing, and R.J. Lefkowitz. 1996. Role of *c-Src* tyrosine kinase in G protein-coupled receptor and $G_{\beta\gamma}$ subunit-mediated activation of mitogen-activated protein kinases. *J. Biol. Chem.* 271:19443–19450.

Marshall, C.J. 1995. Specificity of receptor tyrosine kinase signaling: transient versus sustained extracellular signal-regulated kinase activation. *Cell.* 80: 179–185.

Majno, G., S.M. Shea, and M. Leventhal. 1969. Endothelial contraction induced by histamine-type mediators: an electron microscopic study. *J. Cell Biol.* 42: 647–672.

Michel, C.C. 1992. The transport of albumin: a critique of the vesicular system in transendothelial transport. *Am. Rev. Respir. Dis.* 146:S32–S36.

Michel, C.C., and F.E. Curry. 1999. Microvascular permeability. *Physiol. Rev.* 79:703–761.

Milici, A.J., N.E. Watrous, H. Stukenbrok, and G.E. Palade. 1987. Transcytosis of albumin in capillary endothelium. *J. Cell Biol.* 105:2603–2612.

Murphy, C., R. Saffrich, M. Grummt, H. Gournier, V. Rybin, M. Rubino, P. Auvinen, A. Lutcke, R.G. Parton, and M. Zerial. 1996. Endosome dynamics regulated by a Rho protein. *Nature.* 384:427–432.

Niles, W.D., and A.B. Malik. 1999. Endocytosis and exocytosis events regulate vesicle traffic in endothelial cells. *J. Membr. Biol.* 167:85–101.

Oh, P., D.P. McIntosh, and J.E. Schnitzer. 1998. Dynamin at the neck of caveolae mediates their budding to form transport vesicles by GTP-driven fission from the plasma membrane of endothelium. *J. Cell Biol.* 141:101–114.

Okamoto, T., A. Schlegel, P.E. Scherer, and M.P. Lisanti. 1998. Caveolins, a

family of scaffolding proteins for organizing "preassembled signaling complexes" at the plasma membrane. *J. Biol. Chem*. 273:5419–5422.

Partridge, W.M. 1979. Carrier mediated transport of thyroid hormones through the blood brain barrier: primary role of albumin bound hormone. *Endocrinology*. 105:605–612.

Peters, T., Jr. 1975. Serum albumin. *Adv. Prot. Chem*. 37:161–245.

Qiao, R., A. Siflinger-Birnboim, H. Lum, C. Tiruppathi, and A.B. Malik. 1993. Albumin and *Ricinus communis* agglutinin decrease endothelial permeability via interactions with matrix. *Am. J. Physiol.* 265:C439–C446.

Qiao, R.L., H.S. Yang, W. Yan, L.E. Odekon, P.J. Del Vecchio, T.J. Smith, and A.B. Malik. 1995. Extracellular matrix hyaluronan is a determinant of the endothelial barrier. *Am. J. Physiol.* 269:C103–C109.

Rabiet, M.J., J.L. Plantier, Y. Rival, Y. Genoux, M.G. Lampugnani, and E. Dejana. 1996. Thrombin-induced increase in endothelial permeability is associated with changes in cell-to-cell junction organization. *Arterioscler. Thromb. Vasc. Biol.* 16:488–496.

Rothberg, K.G., Y.-S. Ying, B.A. Kamen, and R.G.W. Anderson. 1990. Cholesterol controls the clustering of the glycophospholipid-anchored membrane receptor for 5-methyltetrahydrofolate. *J. Cell Biol.* 111:2931–2938.

Rothberg, K.G., J.E. Heuser, W.C. Donzell, Y.-S. Ying, J.R. Glenney, and R.G.W. Anderson. 1992. Caveolin, a protein component of caveolae membrane coats. *Cell*. 68:673–682.

Schnitzer, J.E. 1992. Gp60 is an albumin-binding glycoprotein expressed by continuous endothelium involved in albumin transcytosis. *Am. J. Physiol.* 262:H246–H254.

Schnitzer, J.E., and P. Oh. 1994. Albondin-mediated capillary permeability to albumin. Differential role of receptors in endothelial transcytosis and endocytosis of native and modified albumins. *J. Biol. Chem*. 269:6072–6082.

Schnitzer, J.E., W.W. Carley, and G.E. Palade. 1988. Albumin interacts specifically with a 60-kDa microvascular endothelial glycoprotein. *Proc. Natl. Acad. Sci. USA*. 85:6773–6777.

Schnitzer, J.E., P. Oh, E. Pinney, and J. Allard. 1994. Filipin-sensitive caveolae-mediated transport in endothelium: reduced transcytosis, scavenger endocytosis, and capillary permeability of select macromolecules. *J. Cell Biol.* 127: 1217–1232.

Shasby, D.M., and M.W. Peterson. 1987. Effects of albumin concentration on endothelial albumin transport in vitro. *Am. J. Physiol.* 253:H654–H661.

Siflinger-Birnboim, A., F.B. Cooper, P.J. Del Vecchio, H. Lum, and A.B. Malik. 1988. Selectivity of the endothelial monolayer: effects of increased permeability. *Microvasc. Res.* 36:216–227.

Song, K.S., M. Sargiacomo, F. Galbiati, M. Parenti, and M.P. Lisanti. 1997. Targeting of a G alpha subunit (G_{i1} alpha) and c-*Src* tyrosine kinase to caveolae membranes: clarifying the role of N-myristoylation. *Cell Mol. Biol.* 43:293–303.

Tiruppathi, C., A. Finnegan, and A.B. Malik. 1996. Isolation and characterization of a cell surface albumin binding protein from vascular endothelial cells. *Proc. Natl. Acad. Sci. USA*. 93:250–254.

Tiruppathi, C., H. Lum, T.T. Andersen, J.W. Fenton II, and A.B. Malik. 1992. Thrombin receptor 14-amino acid peptide binds to endothelial cells and stimulates calcium transients. *Am. J. Physiol.* 263:L595–L601.

Tiruppathi, C., W. Song, M. Bergenfeldt, P. Sass, and A.B. Malik. 1997. Gp60 activation mediates albumin transcytosis in endothelial cells by a tyrosine kinase-dependent pathway. *J. Biol. Chem*. 272:25968–25975.

Zacchi, P., H. Stenmark, R.G. Parton, D. Orioli, F. Lim, A. Giner, I. Mellman, M. Zerial, and C. Murphy. 1998. Rab17 regulates membrane trafficking through apical recycling endosomes in polarized epithelial cells. *J. Cell Biol.* 140:1039–1053.